

# Modeling and Simulation of Mode Filtered Radio over Multimode Fiber Links

Tamás Cseh, Tibor Berceci, *Life Fellow, IEEE*

**Abstract**—In this paper mode filtered radio over multimode fiber systems are analyzed by simulations. Several mode filters are investigated such as mandrel wrap, air gap mode filter and single mode fiber patchcord. The multimode fibers and the mode filters are modeled, these models are implemented into VPI Transmission Maker and frequency responses are analyzed. According to the frequency responses, EVM analyses are also carried out, and the most advantageous mode filter is selected. All of these mode filters can reduce the effect of the modal dispersion however, their effect is different and their insertion loss is different too. The single mode fiber patchcord is the best choice when modal dispersion is the dominant effect. Mandrel and air gap filter provided better results if the noise is significant.

**Index Terms**—modal dispersion, mode filtering, multimode fiber, radio over fiber, radio over multimode fiber

## I. INTRODUCTION

OPTICAL links are proper solutions for radio signal transmission and distribution, because of the large bandwidth and low attenuation of the optical fiber. The combined optical-radio system, called Radio over Fiber (RoF), is advantageous especially in indoor connections. In a RoF system a central office (CO) is connected to a high number of remote antenna units (RAUs) due to the high number of users. Therefore, the indoor RoF systems are cost sensitive, therefore low cost solutions are necessary. One of the most important ways to reduce the cost of the RoF link is the application of multimode fibers (MMFs). The large core of MMF can reduce the cost of installation, furthermore, older MMF connections could have been found in a lot of buildings and several government offices [1].

The MMFs are reasonable solutions for indoor RoF links, however, MMFs have higher linear distortion effects than single mode fibers (SMF). The main distorting effect is the modal dispersion, which causes bandwidth limitation in the link. The compensation of modal dispersion is an important task, and it is a relevant problem in Radio over Multimode Fiber (RoMMF) systems.

Several methods exist to reduce the effect of the modal dispersion and increase the modal bandwidth. The most important methods are mode filtering [2] and the offset launch

technique [3]. As it is mentioned above, RoMMF concept is cost sensitive, so simple and cheap solutions are preferred to reduce the effect of the modal dispersion. As the offset launch technique demands precise positioning of the light source, it makes the alignment complicated. Hence the mode filtering technique is more practical in RoMMF than the offset launch technique.

Several mode filters exist for different optical applications [4], but they have different effect on modal dispersion. In this paper the investigation of mode filters in RoMMF system is discussed. Three different mode filter types are investigated by simulations: mandrel wrap, air gap mode filter, and single mode fiber patchcord. They have different performance on modal dispersion and insertion loss, so they have different performance on the quality of the communication.

In this paper the performance utilizing mode filters is analyzed. First, the RoMMF link is modeled and this model focuses on modal dispersion. Then, a model of the mode filtered RoMMF with different mode filters is shown. After modeling, we analyze the frequency response of a radio over MMF link and a mode filtered RoMMF link with simulations to show the effects of the mode filters on our proposed system. After the simulation of the frequency responses, the quality of the link is analyzed with several simulation setups. The error vector magnitude (EVM) is investigated with different mode filters, and each mode filter are analyzed at different signal to noise ratios (SNR) and different modulation bandwidths.

## II. SYSTEM MODEL

In this section the model of the RoMMF link is described. First, the total RoMMF link is investigated, then the model of MMF and mode filters are focused. Table I contains the main parameters of the proposed link.

### A. Radio over multimode fiber link model

The radio over fiber system applies subcarrier optical modulation, hence a modulated radio frequency (RF) carrier modulates the light. The RoF systems apply intensity modulation in the optical domain, and direct detection. These systems are called IM-DD. The proposed RoF link applies multimode fiber. The block scheme of a radio over multimode fiber link (RoMMF) is shown in Fig. 1.

The RF signal modulates the intensity of the light. In the proposed model the intensity modulation (IM) is carried out by an external modulator. In order to neglect the nonlinear distortions of the link, the modulator is considered to be linear.

T. Cseh and T. Berceci are with the Department of Broadband Infocommunication and Electromagnetic Theory, Budapest University of Technology and Economics, H-1111 Budapest, Egr̃y József u. 18., Hungary (email: tseh@mht.bme.hu, berceci@hvt.bme.hu)

Practically the external modulators are used in their linear region. Furthermore, in the RoMMF link model the modulator is considered to be chirpless.

Not only the modulator but also the fiber is linear in our system model. If the optical power of the laser is low enough, this consideration is also correct.

Beside the linearity of the link the noise characteristic is also important. Two components add Gaussian white noise to the link: the laser and the photodetector. The laser has relative intensity noise (RIN), and the photodetector generates thermal noise and shot noise. The RoMMF link can be modeled as a linear system with additional Gaussian noise. The block diagram of our RoMMF model is shown in Fig. 2.

The proposed mode filtered system is modeled like the non-mode filtered system. The block diagram of the mode filtered system, and the model of the mode filtered system can be seen in Fig. 3 and Fig. 4, respectively.

To describe the channel, the noise characteristic and the frequency response of the fiber have to be analyzed. In the next sections these two characteristics are modeled.

*B. Frequency response of the RoMMF system*

As it can be seen in Fig. 2, the frequency response of the multimode fiber is an important part of the model. According to [5], the frequency response of the fiber can be written as

$$H_{MMF}(f) = H_{Mod}(f) \cdot H_{Ch}(f), \tag{1}$$

where  $H_{MMF}(f)$  is the frequency response of the MMF,  $H_{Mod}(f)$  is the frequency response of the multimode behavior, and  $H_{Ch}(f)$  is the frequency response of the chromatic behavior of the fiber. According to (1) the frequency response can be separated into two terms: one represents the modal dispersion and the other represents the chromatic dispersion. The chromatic dispersion is caused by the wavelength dependent group delay. The frequency response of the chromatic dispersion can be expressed as follows [6], [7]

$$H_{Ch}(f) = H_{LD}(f) \cdot H_{CS}(f). \tag{2}$$

The chromatic effects can also be separated to two terms: the first term ( $H_{LD}(f)$ ) is caused by spectral linewidth of the laser, and the second term ( $H_{CS}(f)$ ) is the carrier suppression effect which is caused by the optical double side band (ODSB) modulation [7]. These two terms can be written as the following according to [6], [7] and [8]

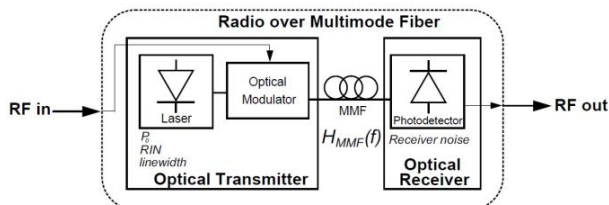


Fig. 1. Block diagram of the RoMMF link

$$H_{LD}(f) = e^{-\frac{1}{2}(D \cdot L \cdot \lambda_0 \cdot f)^2 \left(\frac{\Delta\nu}{f_{opt}}\right)^2}, \tag{3}$$

$$H_{CS}(f) = \cos\left(D \cdot L \cdot \lambda_0 \cdot \pi \cdot \frac{f^2}{f_{opt}^2}\right). \tag{4}$$

If we use the value of  $\Delta\nu$  and  $f_{opt}$  from Table I, (3) can be approximated by one. Similarly, (4) can be also approximated by one, if we consider that the frequency does not exceed 10 GHz. These consideration are real in a RoMMF link. Hence, (3) and (4) can be rewritten as

$$H_{LD}(f) \approx 1, \tag{5}$$

$$H_{CS}(f) \approx 1. \tag{6}$$

As (3) and (4) are approximated by one, (2) leads to the following

$$H_{Ch}(f) \approx 1. \tag{7}$$

Hence, the effect of the chromatic dispersion can be neglected in our proposed system. This consideration is true in practical RoMMF systems, due to the relatively short the fiber length. As a conclusion (1) leads to

$$H_{MMF}(f) \approx H_{Mod}(f). \tag{8}$$

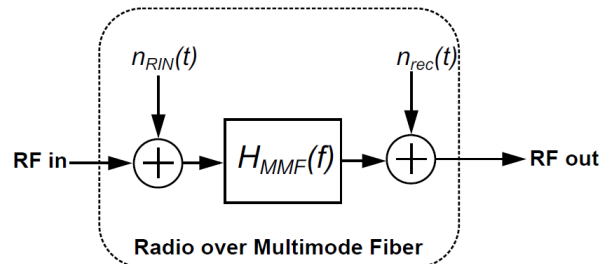


Fig. 2. Linear model of RoMMF.

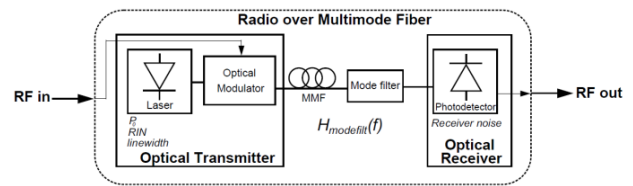


Fig. 3. Block diagram of mode filtered RoMMF

## Modeling and Simulation of Mode Filtered Radio over Multimode Fiber Links

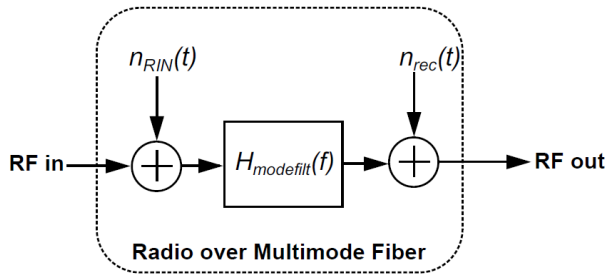


Fig. 4. Model of mode filtered RoMMF link

Therefore, in our proposed RoMMF connection, the modal dispersion is the most significant phenomenon. In the following, the frequency response of the modal behavior is described. The modal dispersion is caused by the different propagation velocity of the modes. In the MMF a lot of modes can propagate, however, several modes propagate with the same velocity and these modes constitute a mode group. The different mode groups propagate with different velocities, and that causes linear distortion, which is called modal dispersion. The total number of mode groups, the delay, the different attenuation of the mode groups, and the coupling between the mode groups influence the modal dispersion and the frequency response of the multimode fiber. The model of the MMF is described by Gloge [9] and Olshansky [10]. This model applies the power flow equation (PFE) [11].

 TABLE I  
PARAMETERS OF THE PROPOSED LINK

| Symbol         | Parameter                              | Value              | Units         |
|----------------|--|--------------------|---------------|
| $n_{core}$     | refractive index of the core           | 1.45               | -             |
| $n_{cladding}$ | refractive index of the cladding       | 1.44               | -             |
| $\Delta$       | refractive index contrast              | 0.0069             | -             |
| $NA$           | numeric aperture of the fiber          | 0.17               | -             |
| $\lambda_0$    | wavelength of the laser                | 1550               | nm            |
| $\Delta\nu$    | linewidth of the laser                 | 10                 | MHz           |
| $RIN$          | relative intensity noise               | -135               | dBc/Hz        |
| $f_{opt}$      | frequency of the optical carrier       | 193.55             | THz           |
| $g$            | refractive index exponent              | 2                  | -             |
| $r_{core}$     | core radius                            | 25                 | $\mu\text{m}$ |
| $r_{cladding}$ | cladding radius                        | 62.5               | $\mu\text{m}$ |
| $h$            | rms height of deformation              | 0.5                | $\mu\text{m}$ |
| $\gamma_0$     | intrinsic fiber attenuation            | 0.2                | dB/km         |
| $C_s$          | mode-coupling constant                 | $6 \times 10^{-5}$ | 1/km          |
| $\rho, \eta$   | fitting constants for mode attenuation | 9, 7.35            | -             |
| $p$            | fitting parameter for mode coupling    | 2                  | -             |
| $\varepsilon$  | modal dispersion parameter             | 0                  | -             |
| $D$            | chromatic dispersion parameter         | 16                 | ps/nm·km      |
| $L$            | length of the fiber                    | 3                  | km            |
| $r_{pD}$       | responsivity                           | 1                  | A/W           |
| $R_L$          | load resistance                        | 50                 | $\Omega$      |
| $T$            | temperature                            | 300                | K             |

$$\frac{\partial P_m}{\partial z} + \tau_m \frac{\partial P_m}{\partial t} = -\gamma_m P_m + d_m (P_{m+1} - P_m) - \frac{m-1}{m} d_{m-1} (P_m - P_{m-1}). \quad (9)$$

In the PFE (9),  $z$  is the length of the fiber,  $t$  is time,  $P_m$  denotes the power of the  $m$ -th mode group, and  $\tau_m$ ,  $d_m$  and  $\gamma_m$  are group delay, attenuation and mode coupling coefficient of the  $m$ -th mode group respectively [11]. Equation (9) can be solved by several methods. In [11] a matrix exponential method is applied, and in this paper this effective calculation is applied. This method calculates the Fourier-transform of (9), and it leads to the following [11]

$$\underline{F}(z) = \exp(\underline{A} \cdot z) \cdot \underline{F}(0), \quad (10)$$

where  $z$  is the length of the fiber,  $\underline{F}(z) = [F_1(z), F_2(z), \dots, F_M(z)]^T$ ,  $M$  is the total number of the mode groups,  $F_m(z)$  is the average power of  $m$ th mode group which is calculated in frequency domain.  $\underline{A}$  is a tridiagonal matrix, which can be expressed as [11]

$$A_{m,m} = -(2\pi \cdot j \cdot f \cdot \tau_m + \gamma_m) - d_m - \frac{m-1}{m} d_{m-1}, \quad (11)$$

$$A_{m,m+1} = d_m, \quad (12)$$

$$A_{m,m-1} = d_{m-1} \frac{m-1}{m}. \quad (13)$$

The key parameters of (9), (11), (12) and (13) can be calculated according to [5] as the following

$$\tau_m = \frac{n_{core}}{c} \left( 1 - \frac{\Delta[4 + \varepsilon]}{g + 2} \cdot \left( \frac{m}{M} \right)^{2g/g+2} \right) \times \quad (14)$$

$$\times \left( 1 - 2\Delta \cdot \left( \frac{m}{M} \right)^{2g/g+2} \right)^{-1/2},$$

$$\gamma_m = \gamma_0 + \gamma_0 \cdot I_\rho \left( \eta \cdot \left( \frac{m-1}{M} \right)^{2g/g+2} \right), \quad (15)$$

$$d_m = C_s \left( \frac{h}{r_{cladding}} \right)^p \left( \frac{r_{core}}{r_{cladding}} \right)^{2p} \left[ \frac{g+2}{g \cdot \Delta} \right]^{1+p} \left( \frac{m}{M} \right)^{-2q}, \quad (16)$$

with

$$q = \frac{[p(g-2)-2]}{g+2}. \quad (17)$$

By calculating  $d_m$ ,  $\tau_m$  and  $\gamma_m$  with substituting the values given in Table I to (14)-(17), we can conclude the following

$$d_m, d_{m-1} \ll \gamma_m, \quad (18)$$

therefore,  $d_m$  can be neglected in our proposed system. Hence  $\underline{A}$  is a diagonal matrix and (11)-(13) is the following

$$A_{m,m} \approx -(2\pi \cdot j \cdot f \cdot \tau_m + \gamma_m), \tag{19}$$

$$A_{m,m+1} \approx 0, \tag{20}$$

$$A_{m,m-1} \approx 0. \tag{21}$$

By replacing (19)-(21) to (10), we get the following expression

$$F_m(z, f) = F_m(0) \cdot e^{-(2\pi j f \tau_m + \gamma_m)z}, \tag{22}$$

and the frequency response of the multimode fiber can be calculated according to [11]

$$H_{Mod}(f) = \frac{\sum_{m=1}^M m \cdot F_m(z, f)}{\sum_{m=1}^M m \cdot F_m(0, f)}. \tag{23}$$

Equation (23) can be rewritten to another form, which contains the power of  $m$ -th mode group, and the total input power ( $P_0$ )

$$H_{MMF}(f) = \frac{1}{P_0} \sum_{m=1}^M P_m e^{-(2\pi j f \tau_m + \gamma_m)z}. \tag{24}$$

Equation (24) is the frequency response of radio over multimode fiber system, when the mode coupling can be neglected. As we have seen it above, this approximation is correct for our proposed system due to their parameters. Furthermore, (24) shows that the frequency response depends strongly on  $P_m$ , this way the influence of the input power distribution of the mode groups is very high. The input power distribution depends on the launch condition at the input of the fiber. Two types of launch conditions are tested in this paper: overfilled launch condition (OFL) and restricted mode launch (RML). The OFL is an important launch condition, because it shows a theoretically worst case of the modal behavior, and the launch condition of some practical RoMMF (which applies LEDs) connections can be considered as OFL as well. The OFL means that all of the modes are generated equally. If we know which modes belong to which mode group, the power distribution of the mode groups can be calculated. This calculation is well known [3], [4], [5].

The RML means that restricted number of modes are generated at the input. The RML is typical at laser-fiber interfaces. The power distribution which is caused by RML can be calculated by using overlap integral [3], [4], [12]. The overlap integral calculates the coupling between the laser modes and the modes of the MMF. To decide which modes belong to which mode group in the case of RML, the calculation which are mentioned in the case of OFL should be applied [3], [4], [5].

*C. Frequency response of the mode filtered RoMMF system*

The mode filters can reduce the number of the mode groups and this effect will cause reduction in the effect of the modal

dispersion. Each of the mode filters produces different attenuation for the mode groups, and the attenuation characteristics are also different for different mode filters. In this paper three mode filters are investigated in the RoMMF system: air gap filter, mandrel wrap, and SMF patchcord.

The air gap mode filter contains two multimode fibers coupled to each other with a small air gap. For the size of the gap 1 mm is taken in this paper. At the transmitter fiber end the light radiates out from the fiber. The diverged laser beam radiated out of the transmitter fiber, generates several modes in the other fiber at the receiver side. However, the diverged laser beam can generate restricted number of modes at the receiver fiber end of the air gap filter. Hence, the higher order modes are filtered off by the air gap [4], [12]. The mode filtering effect depends on the size of the gap: longer gap causes stronger filtering effect, but the attenuation will be higher as well. According to [4] the air gap filter with 1 mm gap size attenuates almost all of the mode groups except few lower order modes.

With a few turns of the fiber on a reel with small diameter, the higher order modes are filtered off [2]. This mode filter is called mandrel wrap. There is a radiation loss due to the turns on the reel, and the radiation loss is different for each mode group. The higher order modes are radiated stronger than the lower order ones. This effect depends on the reel diameter [4]. With a standard reel diameter of the mandrel wrap the half of the mode groups can be filtered off [2], [4].

The function of the SMF patchcord as a mode filter is the following: through the SMF patchcord only the fundamental mode can propagate due to its smaller core size. Except the fundamental mode all the modes are filtered off, but it cause relatively high insertion loss [2]. By applying a SMF patchcord as mode filter, the effect of the modal dispersion can be eliminated, and the frequency response of the mode filtered RoMMF could be perfectly flat. The mode filtering effect of the SMF patchcord is investigated in several papers such as [13], [14].

To describe the mode filtered RoMMF, the frequency response equation of RoMMF is used. As it was mentioned above, the mode filters can attenuate the different mode groups differently, so with some modifications in (24) the frequency response of the mode filtered RoMMF is given as the following

$$H_{Modfilt}(f) = \frac{1}{P_0} \sum_{m=1}^M \alpha_m P_m e^{-(2\pi j f \tau_m + \gamma_m)z}, \tag{25}$$

where  $\alpha_m$  is the attenuation of a given mode filter on the  $m$ -th mode group. Equation (25) gives the frequency response of the mode filtered RoMMF and (24) gives the frequency response of the RoMMF without mode filtering. If the parameters of (24) and (25) are well known, the frequency responses can be calculated. In this paper the values of  $\alpha_m$  are calculated by applying the results of [4].

## Modeling and Simulation of Mode Filtered Radio over Multimode Fiber Links

## D. Noise behavior of the proposed system

After the description of the frequency response of the RoMMF and the mode filtered RoMMF, the noise behavior should be analyzed. As it could be seen in Fig. 2 and Fig. 4, there are additive noise at both sides of the link. At the transmitter side the noise comes from the relative intensity noise (RIN) of the laser. The RIN can be calculated in the electrical domain as the following

$$\frac{\langle i_{RIN} \rangle}{\sqrt{B}} = P_0 \cdot r_{PD} \sqrt{RIN}, \quad (26)$$

where  $P_0$  is the optical power of the laser  $r_{PD}$  is the responsivity of the photodetector, RIN is the relative intensity noise,  $B$  is the bandwidth, and  $\langle i_{RIN} \rangle$  is the average noise current of the RIN at the photodetector.

At the receiver side of the link, the noise comes from the photodiode. The receiver noise has two components: the shot noise and thermal noise. If a PIN diode is applied as a receiver, the shot noise and thermal noise can be expressed, respectively [15]

$$\frac{\langle i_{shot} \rangle}{\sqrt{B}} = \sqrt{2 \cdot q \cdot P_0 \cdot r_{PD}}, \quad (27)$$

$$\frac{\langle i_{thermal} \rangle}{\sqrt{B}} = \sqrt{\frac{4 \cdot k \cdot T}{R_L}}, \quad (28)$$

where  $q$  is the elementary charge,  $T$  is the temperature,  $R_L$  is the load resistance, and  $k$  is the Boltzmann-constant. As RIN is relatively low in our proposed system (Table I) and  $P_0$  is also low enough, the thermal noise will be the most dominant noise effect. In this paper the noise level is fixed, but the analysis is made at different signal power levels, so our proposed system is simulated at different signal to noise ratios (SNR).

After the description of the noise behavior and the frequency response of the RoMMF system, the linear model of the RoMMF link is determined. All of the parameters are given for the simulations of the RoMMF link in Table I.

TABLE II  
CALCULATED PARAMETERS FOR SIMULATIONS

| $m$ | $\Delta\tau_m [ps]$ | $\gamma_m [km^{-1}]$   | $P_m/P_0$ |      |     | $\alpha_m$ |    |
|-----|---------------------|------------------------|-----------|------|-----|------------|----|
|     |                     |                        | OFL       | RML  | a)  | b)         | c) |
| 1   | 0                   | $4.61 \times 10^{-2}$  | 0.04      | 0.11 | 1   | 1          | 1  |
| 2   | 0.0043              | $4.61 \times 10^{-2}$  | 0.04      | 0    | 1   | 0.5        | 0  |
| 3   | 0.011               | $4.61 \times 10^{-2}$  | 0.08      | 0.35 | 1   | 0.44       | 0  |
| 4   | 0.021               | $4.61 \times 10^{-2}$  | 0.08      | 0    | 1   | 0.38       | 0  |
| 5   | 0.034               | $4.63 \times 10^{-2}$  | 0.12      | 0.34 | 0.5 | 0.31       | 0  |
| 6   | 0.05                | $4.86 \times 10^{-2}$  | 0.12      | 0    | 0   | 0.25       | 0  |
| 7   | 0.069               | $6.17 \times 10^{-2}$  | 0.16      | 0.16 | 0   | 0.18       | 0  |
| 8   | 0.09                | $12.05 \times 10^{-2}$ | 0.16      | 0    | 0   | 0.1        | 0  |
| 9   | 0.115               | $32.67 \times 10^{-2}$ | 0.2       | 0.04 | 0   | 0          | 0  |

a) mandrel wrap, b) air gap filter c) SMF patchcord.

## III. SIMULATION RESULTS

In the former sections the model of the RoMMF and the calculations are described, hence, the calculated parameters are available for the simulation setup. Two parts of the simulation results are presented: in the first part the frequency responses are analyzed and in the second part EVM simulations are investigated. To simulate the frequency responses, the main parameters of (24) and (25) should be calculated. First the number of the mode groups ( $M$ ) has to be determined. According to [5] the number of mode groups can be expressed as the following

$$M = 2\pi \cdot r_{core} \frac{n_{core}}{\lambda} \left( \frac{g \cdot \Delta}{g + 2} \right)^{1/2}. \quad (29)$$

By using (29) we got  $M=9$ . Hence, the main parameters of the MMF and mode filters should be calculated for nine mode groups. The calculated parameters are summarized in Table II.

## A. Simulation of frequency responses

When the parameters are well known, the frequency response of RoMMF and mode filtered RoMMF can also be calculated. The frequency responses are obtained for both OFL and RML. These results are plotted in Fig. 5 and Fig. 6, respectively. The OFL frequency response without mode filtering has two notches up to 10 GHz at around 3 GHz and around 5.4 GHz. The mandrel shifts the latter notch, but this notch is also relatively strong. The air gap filter makes the frequency response smoother. The trace is not flat, however, the transmission level at the notches is smaller than in the case of the mandrel. Due to the smoother characteristics we expect better performance for air gap filter than mandrel. As the SMF patchcord filters off all of the mode groups except the fundamental mode, a totally flat characteristic is expected. The simulation results show totally flat frequency response with

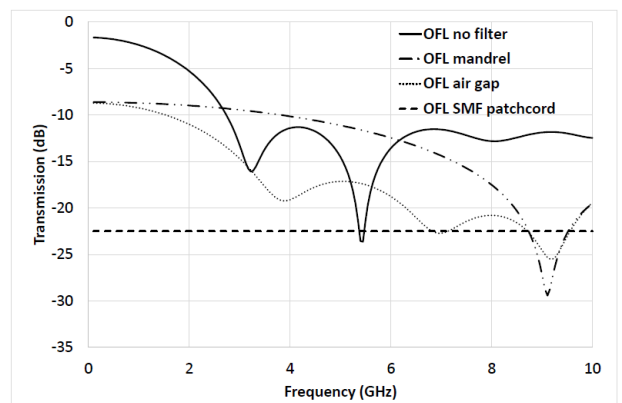


Fig. 5. Frequency responses of RoMMF with different mode filters for OFL

SMF patchcord for OFL condition.



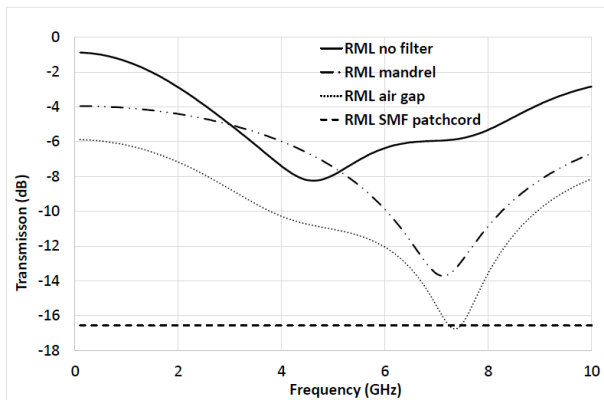


Fig. 6. Frequency responses of RoMMF with different mode filters with RML

For RML condition the frequency response without mode filtering has only one notch around 4.5 GHz, but the level of this notch is smaller than in the case of OFL condition. For RML the air gap and mandrel filtering show small difference. Both of the frequency response traces are almost the same, they have one notch, and the shape of the traces are really similar, hence, almost the same performance is expected for air gap and mandrel filter for RML condition.

The SMF patchcord has totally flat frequency response for both of the launch conditions, but its insertion loss is different for the two launch conditions. For OFL the insertion loss (IL) is around 22dB and for RML it is 16dB. Basically, the insertion losses of mandrel and air gap filter behave similarly to each other in case of both launch types. SMF patchcord has higher insertion losses compared to mandrel and air gap filter which is around 10dB. The insertion losses (IL) of the filters are summarized in Table III. The IL is very important, because of higher IL the signal to noise ratio (SNR) is more significant. Therefore, the SMF patchcord is the most sensitive for SNR, however, it can eliminate most of the modal dispersion effect, as the SMF patchcord can produce flat frequency response. As the efficiency of the mode filters depend on the frequency response and the SNR level together, in the following, the mode filters are compared to each other with different SNR. In order to compare the mode filters with different SNR, modulated signals are used, and the EVM is analyzed. The EVM analysis can show a better comparison for the performance of the mode filters, as a result, the best mode filters can be found for each of the RoMMF setups.

*B. EVM analysis*

For EVM analysis, a modulated signal is applied at a certain carrier frequency. In this paper QPSK modulation is used for EVM analysis, and the carrier frequency is set to notch frequencies: for OFL the carrier frequency is 5.42 GHz, and for RML it is 4.5 GHz. At the notch frequencies the effect of the modal dispersion is the strongest, so it is worth to analyze the mode filtering effect at these worst case frequencies. As it is mentioned in above, the EVM investigation is made at two different SNR to analyze the performance of the link. The higher SNR is 40dB and the lower SNR is 30dB. These SNR

TABLE III  
INSERTION LOSS (IL) OF DIFFERENT MODE FILTERS

|               | OFL-IL(dB) | RML-IL(dB) |
|---------------|------------|------------|
| no filter     | 1.66       | 0.87       |
| mandrel       | 8.61       | 3.95       |
| air gap       | 8.7        | 5.85       |
| SMF patchcord | 22.5       | 16.56      |

values are considered at the transmitter side. Although, the performance of the link is usually determined by SNR at receiver side, however, the SNR at the receiver side can be different for different mode filtering setups. The mode filters have different insertion losses (Table III), furthermore, the insertion losses depend on the carrier frequencies (Fig. 5 and Fig. 6). Consequently, it is easier to use the SNR at the transmitter side.

The quality of the transmission depends on the modulation bandwidth. The effect of modal dispersion is higher for higher modulation bandwidth, therefore, the EVM is simulated at different modulation bandwidths as well. The simulations are carried out by using VPI Transmission Maker 9.2 [15]. The model of the mode filtered RoMMF links are implemented to VPI according to the calculations, which are described above. The EVM analysis is carried out for different SNR and for both OFL and RML. First, the EVM results are plotted for OFL at higher SNR in Fig 7.

In this case, the SNR is relatively high, so the dominant distortion effect is the modal dispersion. The best mode filter is the SMF patchcord, and its performance is especially impressive at higher modulation bandwidth. At 500MHz the effect of the SMF patchcord is improved to 1.5%. The air gap filter has worse performance than the SMF patchcord and better performance than the mandrel filter. This experiences are agreed with the results of frequency responses.

At lower SNR the modal dispersion is not the only significant distortion effect, the noise can also limit the quality of the channel. The EVM results are plotted for OFL at lower SNR in Fig 8.

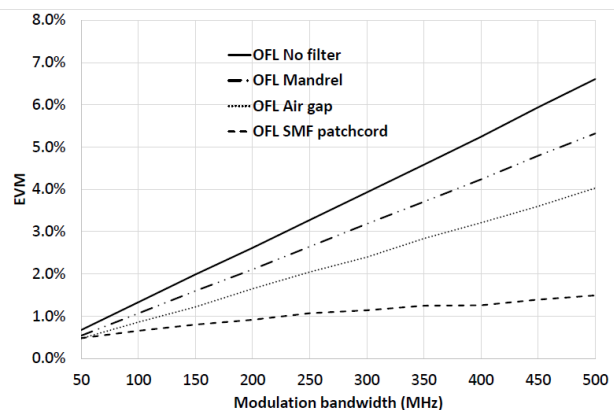


Fig. 7. Modulation bandwidth vs. EVM for OFL at higher SNR

Modeling and Simulation of Mode Filtered Radio over Multimode Fiber Links

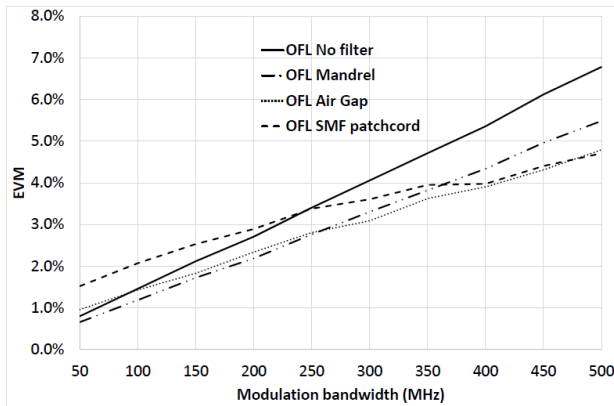


Fig. 8. Modulation bandwidth vs. EVM for OFL at lower SNR

In this case, the SMF patchcord is not effective enough especially at smaller bandwidth. When the modulation bandwidth is even higher, the modal dispersion affects the transmission more, so the performance of the SMF patchcord increases, but it is not as advantageous as at higher SNR. The air gap mode filter gives similar results: at higher modulation bandwidths, the air gap mode filter improves the quality of communication stronger than at lower modulation bandwidths. However, the mandrel have better performance at both lower and higher modulation bandwidths for OFL. As the mandrel is less sensitive to noise, due to its lower insertion loss, the mandrel can be a suitable type of mode filter at lower SNR for OFL.

When RML is applied the insertion losses of the mode filters are smaller (Table III), so the mode filters have different behavior. At higher SNR the results are shown in Fig. 9. As it can be seen, the mandrel and the air gap filter have almost the same performance. At 500 MHz modulation bandwidth the air gap improves the EVM from 5.5% to 5%, and the mandrel can improve the EVM to 4.5%. However, the SMF patchcord shows much better performance. When the link is mode filtered with SMF patchcord, the EVM is decreased to 0.9%. Hence, for RML at higher SNR the best mode filter is SMF patchcord.

At lower SNR the mode filters with higher insertion loss can be less advantageous. However, by applying RML launch

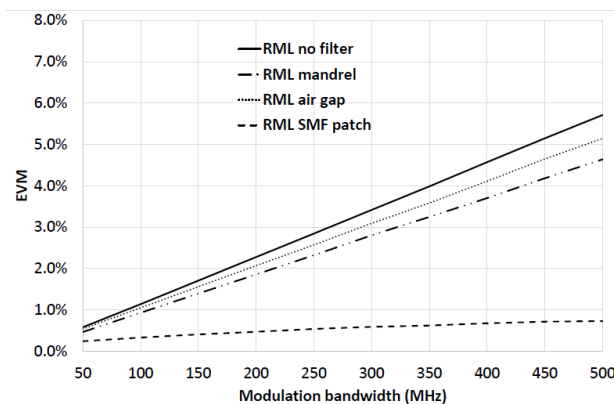


Fig. 9. Modulation bandwidth vs. EVM for RML at higher SNR

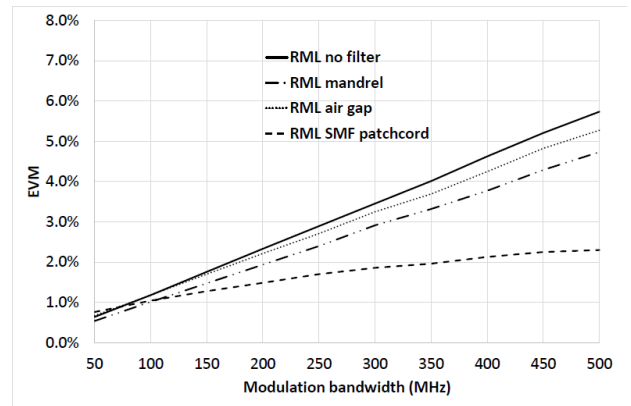


Fig. 10. Modulation bandwidth vs. EVM for RML at lower SNR

condition the insertion loss of the mode filters is much smaller than in the other case, when launch condition is OFL. At lower SNR with RML the results are shown in Fig. 10. In this case the SMF patchcord can reduce the EVM, but this improvement is smaller at lower SNR than at higher SNR. At lower SNR for RML the best mode filter is still SMF patchcord, because the mandrel and air gap filter cannot improve the quality of the communication as much as the SMF patchcord and the air gap mode filter and mandrel have almost the same performance. Thus, according to Fig. 10 the best mode filter for RML at lower SNR is the SMF patchcord, especially for higher modulation bandwidth.

By analyzing the EVM, the best mode filters for different RoMMF scenarios can be selected. These results are summarized in Table IV. It shows that for RML, the SMF patchcord is the best choice, however, for OFL the SMF patchcord shows better performance, when the SNR is high enough. On the other hand, at lower SNR, the mandrel and air gap filter could be a more advantageous choice than SMF patchcord.

TABLE IV  
MODE FILTER SUMMARY

|                           | OFL           |                 | RML           |               |
|---------------------------|---------------|-----------------|---------------|---------------|
|                           | High SNR      | Low SNR         | High SNR      | Low SNR       |
| Low Modulation bandwidth  | SMF patchcord | Mandrel/Air gap | SMF patchcord | SMF patchcord |
| High Modulation Bandwidth | SMF patchcord | Mandrel/Air gap | SMF patchcord | SMF patchcord |

IV. CONCLUSION

To summarize, mode filtered radio over multimode fiber systems are investigated by simulations in this paper. The frequency response of the mode filtered RoMMF is modeled and simulated in order to find the most efficient mode filter at different RoMMF scenarios. Three different types of mode filters are analyzed in RoMMF: mandrel, air gap filter and SMF patchcord. Not only the frequency responses but also the EVM are simulated. The analysis is carried out for different launch conditions (OFL and RML) at different SNR level. The

frequency responses show that the SMF patchcord can eliminate the modal dispersion, but its insertion loss is also the highest. For OFL the insertion loss is higher than for RML, because for OFL the number of the mode groups are higher than for RML, and they do not propagate only around the center of the fiber, hence the mode filters can attenuate higher number of mode groups for OFL than for RML, which leads to higher insertion losses for the case of OFL.

The EVM analysis shows that SMF patchcord can be the best solution at higher SNR, and it could work fine at lower SNR as well, if the launch condition is RML. For OFL, at lower SNR, mandrel and air gap mode filter show better performance than the SMF patchcord. To conclude, if the launch condition is considered to be RML in a RoMMF system, the SMF patchcord is the best choice for mode filtering, especially at higher modulation bandwidth. At other scenarios mandrel or air gap filter can also shows advantageous behavior.

REFERENCES

[1] T. Cseh, E. Udvary, "Cost effective RoF with VCSELs and Multimode Fiber," in *16th European Conference on Networks and Optical Communications (NOC)*, Newcastle upon Tyne, UK, 2011, pp. 60-63.

[2] J. Siuzdak, G. Stepniak, "Influence of modal filtering on the bandwidth of multimode optical fibers," *Optica Applicata*, vol. 37, no. 1-2, pp. 31-39, 2007.

[3] L. Raddatz, I. H. White, D. G. Cunningham, M. C. Nowell, "An Experimental and Theoretical Study of the Offset Launch Technique for the Enhancement of the Bandwidth of the Multimode Fiber Links," *Journal of Lightwave Technology*, vol. 16, no. 3, pp. 324-331, March, 1998.

[4] A. G. Hallem, "Mode Control in Multimode Optical Fibre and its Applications," PhD dissertation, Aston University, 2007.

[5] G. Yabre, "Comprehensive Theory of Dispersion in Graded-Index Optical Fibers," *Journal of Lightwave Technology*, vol. 18, no. 2, pp. 166-177, February, 2000.

[6] I. Gasulla, J. Capmany, "RF transfer function of analogue multimode fiber using an electric field propagation model: Application to Broadband Radio over fiber systems," in *International Topical Meeting on Microwave Photonics*, Grenoble, France, 2006, pp. 1-4.

[7] D. S. Montero, I. Gasulla, I. Möllers, D. Jäger, J. Capmany, "Experimental Analysis of Temperature Dependence in Multimode Fiber Optical Links for Radio-over-Fiber Applications," in *17th International Conference on Transparent Optical Networks*, Sao Miguel, Azores, Portugal, 2009, pp. 1-4.

[8] L. A. Neto, D. Erasme, N. Genay, P. Chanclou, Q. Deniel, F. Traore, T. Anfray, R. Hmadou, C. Aupetit-Berthelemot, "Simple Estimation of Fiber Dispersion and Laser Chirp Parameters Using the Downhill Simplex Fitting Algorithm," *Journal of Lightwave Technology*, vol. 31, no. 2, pp. 334-342, January, 2013.

[9] D. Glöge, "Optical Powerflow in Multimode Fibers," *The Bell System Technical Journal*, vol. 51, no. 8, pp. 1767-1783, October, 1972.

[10] R. Olshansky, "Mode Coupling Effects in Graded-Index Optical Fiber," *Applied Optics*, vol. 14, no. 4, pp. 935-945, 1975.

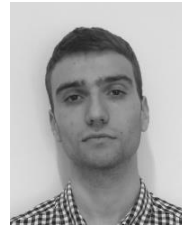
[11] G. Stepniak, J. Siuzdak, "An efficient method for calculation of the MM Fiber frequency response in the presence of mode coupling" *Optical and Quantum Electronics*, vol. 38, no. 15, pp. 1195-1201, December, 2006

[12] P. Pepeljugoski, S. E. Golowich, A. J. Ritger, P. Kolesar, A. Risteski, "Modeling and Simulation of Next-Generation Multimode Fiber Links," *Journal of Lightwave Technology*, vol. 21, no.5, pp. 1242-1255, May, 2003.

[13] T. Cseh, T. Berceli: "Improved Receiver Techniques for Radio over Multimode Fiber Systems." *18th European Conference on Networks and Optical Communications (NOC)*, Graz, Austria, 2013, pp. 23-26.

[14] T. Cseh, T. Berceli: "Dispersion compensation in millimeter wave radio over fiber systems" *Microwave and Optical Technology Letters*, vol. 57, no. 1, pp. 204-207, January, 2015.

[15] VPI Transmission maker/VPI component maker, user's manual, May 2014



**Tamás Cseh** received the B.S. and M.S. degrees in electric engineering from the Budapest University of Technology and Economics. He started his Ph.D. studies in 2011, and he is currently a Research Assistant at Budapest University of Technology and Economics, Department of Broadband Infocommunication and Electromagnetic Theory. His interest includes optical communication with multimode fibers, and radio over fiber systems and dispersion compensation methods. He has authored and co-authored about 15 papers. Mr. Cseh is a member of Scientific Association for Infocommunications, Hungary (HTE)



**Tibor Berceli** graduated in electrical engineering at the Technical University of Budapest. He received the Doctor of Technical Science (D.Sc.) degree from the Hungarian Academy of Sciences. Dr. Berceli is Professor of Electrical Engineering at the Budapest University of Technology and Economics

As a researcher he worked on surface wave transmission lines, dielectric waveguides, several kinds of microwave semiconductor oscillators and amplifiers, parametric circuits, up- and down-converters, injection locked oscillators, etc.

His present field of interest is the combined optical-microwave circuits and systems. He initiated a new lightwave-microwave phase detector, and new mixing processes. He suggested new approaches for optical millimeter wave generation and sub-carrier optical transmission. Prof. Berceli is Life Fellow of IEEE. He is the author of 226 papers and 6 books published in English. He presented 96 papers at international conferences. Dr. Berceli was visiting professor at universities in the USA, UK, Germany, Japan, France, Finland and Australia